Published online 15 November 2011 *Nucleic Acids Research, 2012, Vol. 40, No. 5* ***2357–2367***
doi:10.1093/nar/gkr980

Development of a 'clickable' non-natural nucleotide to visualize the replication of non-instructional DNA lesions

Edward A. Motea[1], Irene Lee[1] and Anthony J. Berdis[2,*]

[1]Department of Chemistry and [2]Department of Pharmacology, Case Western Reserve University, Cleveland, OH 44106, USA

Received August 31, 2011; Revised October 11, 2011; Accepted October 14, 2011

ABSTRACT

The misreplication of damaged DNA is an important biological process that produces numerous adverse effects on human health. This report describes the synthesis and characterization of a non-natural nucleotide, designated 3-ethynyl-5-nitroindolyl-2′-deoxyriboside triphosphate (3-Eth-5-NITP), as a novel chemical reagent that can probe and quantify the misreplication of damaged DNA. We demonstrate that this non-natural nucleotide is efficiently inserted opposite an abasic site, a commonly formed and potentially mutagenic non-instructional DNA lesion. The strategic placement of the ethynyl moiety allows the incorporated nucleoside triphosphate to be selectively tagged with an azide-containing fluorophore using 'click' chemistry. This reaction provides a facile way to quantify the extent of nucleotide incorporation opposite non-instructional DNA lesions. In addition, the incorporation of 3-Eth-5-NITP is highly selective for an abasic site, and occurs even in the presence of a 50-fold molar excess of natural nucleotides. The biological applications of using 3-Eth-5-NITP as a chemical probe to monitor and quantify the misreplication of non-instructional DNA lesions are discussed.

INTRODUCTION

Cellular DNA is frequently damaged by exposure to a wide variety of internal and external DNA damaging agents. While the resulting DNA lesions can be repaired by several independent pathways (1), they are also inappropriately replicated by DNA polymerases in a complex biological process known as **t**rans**l**esion DNA **s**ynthesis (TLS) (2). TLS can cause increased levels of mutagenesis that can in turn spark the development of diseases such as cancer. Despite the biological importance and medical ramifications of TLS, relatively little is known regarding the cellular mechanisms by which DNA polymerases misreplicate DNA lesions.

Abasic sites are one of the most commonly formed DNA lesions that can be misreplicated to cause mutagenesis (3). These non-instructional DNA lesions form spontaneously at rates ranging between 10 000 and 200 000 per day per cell (4,5). In addition, DNA damaging agents such as temozolomide which are used in cancer chemotherapy (6) can significantly increase the rates of their formation. While abasic sites lack templating information, most high-fidelity DNA polymerases preferentially incorporate dATP opposite this lesion (7,8). This unusual specificity in nucleotide selection is commonly referred to as the 'A-rule' and could account for the mutagenic potential of this non-instructional lesion (9,10). Surprisingly, members of Y-family DNA polymerases do not obey the 'A-rule'. For example, Rev1 inserts dCTP opposite abasic sites with a higher catalytic efficiency than dATP, dGTP, or dTTP (11). In this case, dCTP incorporation is mediated by interactions of the incoming nucleotide with an active site arginine residue. However, not all 'specialized' polymerases show this preference. A recent report by Choi *et al.* (12) demonstrated that other specialized DNA polymerases such as pol κ insert dCTP and dATP opposite this lesion, while pol η preferentially inserted dTTP and pol ι inserted dTTP, dGTP and dATP.

To investigate the molecular basis for the 'A-rule' catalyzed by high-fidelity polymerases, we developed a series of non-natural nucleotides that mimic dATP and characterized their incorporation opposite DNA containing a tetrahydrofuran moiety which is a stable and non-reactive mimetic for an abasic site (Figure 1A) (13–17). One particular analog, designated 5-nitroindolyl-2′-deoxynucleoside triphosphate (5-NITP) (Figure 1B), is noteworthy as it is incorporated opposite an abasic site with an incredibly high catalytic efficiency (k_{pol}/K_d) of

*To whom correspondence should be addressed. Tel: +1 216 368 4723; Fax +1 216 368 3395; Email: ajb15@cwru.edu

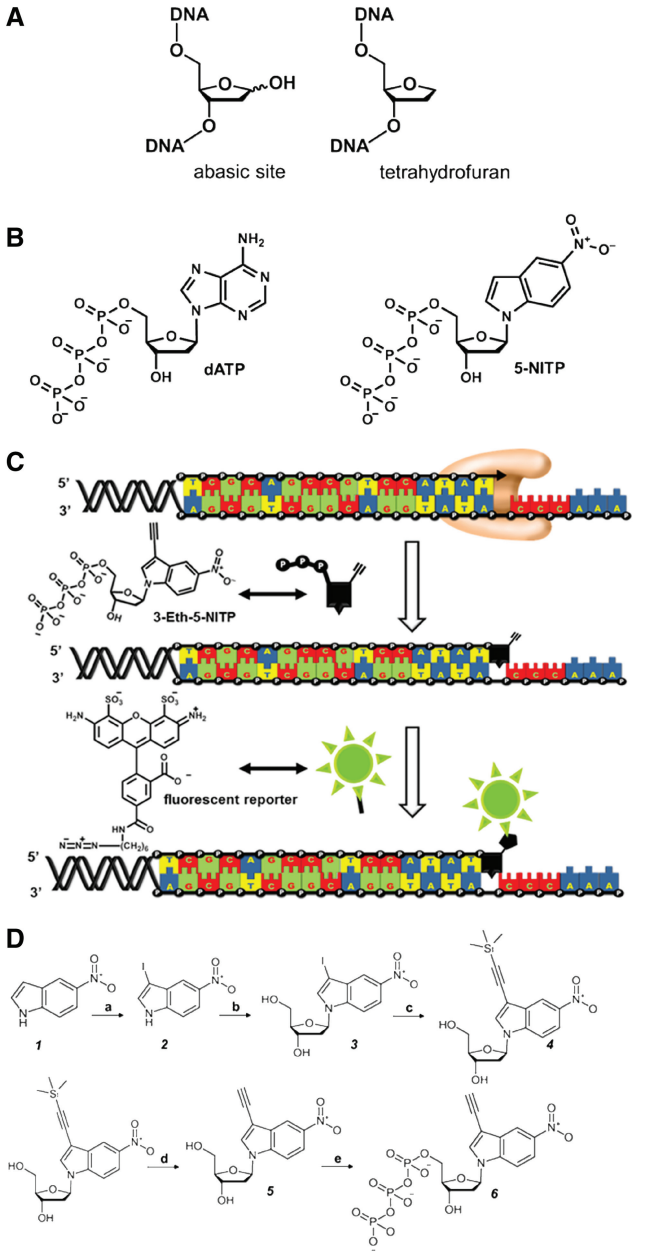

Figure 1. Non-natural nucleotides as probes for TLS. (**A**) Comparison of the structures for an abasic site with that for a tetrahydrofuran moiety, the stable and non-reactive mimetic for an abasic site. (**B**) Structures of dATP and 5-NITP, a prototypical non-natural nucleotide that is selectively and efficiently incorporated opposite an abasic site. (**C**) Strategy for using 'clickable' nucleotides to monitor TLS. (**D**) Synthesis of 3-Eth-5-NITP using the following reagents and conditions: (**a**) I_2, KOH, DMF (**b**) *i.* NaH, 1-α-chloro-3,5-di-(*O*-*p*-toluoyl)-2-deoxy-D-ribose, anhydrous ACN, RT, 16 h; *ii.* NaOMe, MeOH, pH > 12, RT, 16 h; (**c**) $Pd(PPh_3)_2Cl_2$, CuI, triethylamine, trimethylsilylacetylene, anhydrous THF, RT, 3 h; (**d**) 1 M TBAF, THF, RT, 3 h; (**e**) *i.* $POCl_3$, Proton Sponge®, trimethylphosphate, 0°C; *ii.* Tributylammonium pyrophosphate, DMF, tributylamine, RT, 15 min; *iii.* 1 M TEAB, RT, 2 h.

$10^6\,M^{-1}\,s^{-1}$ by the high-fidelity bacteriophage T4 DNA polymerase (13,14). This k_{pol}/K_d value is ~1000-fold higher than dATP, the preferred natural nucleotide substrate (18). Subsequent crystal structures of an exonuclease deficient variant of analogous DNA polymerase from bacteriophage RB69 showed that the non-natural nucleotide existed in an interhelical configuration when paired opposite the lesion (19). This thermodynamically favored configuration explains the enhanced kinetics of 5-NITP as the nucleotide is stabilized by dipole-induced stacking interactions between the 5-nitro group and the nucleobase that is 3′ to the lesion. Equally important, this nucleotide analog is poorly inserted opposite any of the four natural nucleobases, displaying low catalytic efficiencies of $>10^3\,M^{-1}s^{-1}$ (13,14). In fact, 5-nitroindole was initially reported as a 'universal nucleobase' due to its ability to indiscriminately pair with each of the four natural nucleobases as defined by duplex melting experiments (20). However, while 5-nitroindole can indiscriminately pair with natural nucleobases, the corresponding nucleoside triphosphate was poorly incorporated opposite unmodified DNA (21,22). Indeed, our results showing that 5-NITP is incorporated opposite non-instructional DNA lesions with very high efficiencies (14) suggested that it could be further developed as a chemical probe to quantify the replication of this lesion. In addition, the high selectivity of this analog for damaged DNA could be used to differentiate replication of the lesion from that of normal DNA synthesis. This report provides a detailed analysis for the conversion of 5-NITP into a chemical probe that can visualize and quantify TLS. This was achieved using 'click' chemistry (23,24) to selectively introduce an ethynyl moiety at the 3-position of 5-NITP so that it can be tagged with a fluorogenic reporter after it is incorporated opposite a DNA lesion (Figure 1C).

MATERIAL AND METHODS

Materials

Potassium hydroxide, iodine, copper iodide, 1 M tetrabutylammonium fluoride (TBAF) in THF, 5-nitroindole, trimethylsilylacetylene, anhydrous sodium methoxide, phosphoryl oxychloride, *bis*(triphenylphosphine) palladiumchloride $[Pd(PPh_3)_2Cl_2]$ and 1,8-*bis* (dimethylamino)naphthalene (Proton Sponge) were purchased from ACROS. Sodium hydride (60% dispersion in mineral oil), tributylammonium pyrophosphate, anhydrous dimethyl formamide (DMF) and dimethoxyethane (DME) were purchased from Sigma-Aldrich. Triethylammonium bicarbonate (TEAB) was prepared as previously described (25). Trimethylphosphate and tributylamine were purified via fractional distillation under reduced pressure. All anhydrous solvents were dried over 4 Å molecular sieves and stored under argon after purification. Acetonitrile was purified by refluxing with CaH_2 for 2 h followed by simple distillation. All other solvents and reagents used were purchased at the highest purity. Water-sensitive reactions were performed in oven-dried glassware under argon. The intermediates and products were characterized by NMR, UV–vis absorbance, and mass spectrometry. ^1H, ^{13}C and ^{31}P NMR spectra were recorded in a Varian-400 FT NMR spectrometer. All chemical shifts are reported

in ppm and the coupling constants are in Hertz. ^{1}H and ^{13}C NMR spectra were taken in deuterated dimethylsulfoxide (DMSO-d_6) using tetramethylsilane (TMS) as the external reference and DMSO as the internal standard. ^{31}P-NMR spectra were taken in D_2O with 50 mM Tris–HCl and 2 mM EDTA. Phosphoric acid (85%) was used as the external standard. High-resolution electrospray ionization mass spectrometry (Hi-Res ESI–MS) was performed on an IonSpec HiRes ESI-FTICRMS at the University of Cincinnati Mass Spectrometry facility. The configuration of the nucleoside was confirmed by ^{1}H NMR NOE difference spectroscopy on a Varian Inova 600 NMR instrument. Thin layer chromatography was carried out on a Whatman Silica Gel UV_{254} plates. Column chromatography was performed on a Fisher Scientific Silica Gel, sizes 32–63. HPLC analysis and purification were performed using a JASCO Model PU-2089 instrument with reverse phase C-18 Vydac columns. UV absorption of the nucleosides was used for their quantification and was performed on a Cary 50 spectrophotometer.

Magnesium acetate, $MgCl_2$ and Trizma base were from Sigma. [γ-^{32}P]-ATP was purchased from Perkin Elmer, Inc. (Boston, MA, USA). Urea, acrylamide and bis-acrylamide were from National Diagnostics (Rochester, NY, USA). All oligonucleotides were synthesized by Operon Technologies (Alameda, CA, USA). Oligonucleotides were purified as previously described (26) using denaturing polyacrylamide gel electrophoresis for single-stand DNA and native polyacrylamide gel electrophoresis for duplex DNA. All other materials were obtained from commercial sources and were of the highest quality available. The exonuclease-deficient mutant of the bacteriophage T4 DNA polymerase was purified and quantified as previously described (26,27).

Preparation of 3-iodo-5-nitroindole (2)

A solution of I_2 (830 mg, 3.25 mmol) in anhydrous DMF (8 ml) was added into a solution of 5-nitroindole (**1**) (500 mg, 3.10 mmol) and KOH (440 mg, 7.75 mmol) in DMF (8 ml) at room temperature and stirred for 1.5 h under argon. The reaction mixture was immediately poured into water (200 ml) containing ammonia (0.5%) and sodium metabisulphite (0.1%) chilled at 0°C. The resulting precipitate was vacuum filtered and washed with cold water and vacuum dried in a desiccator overnight. The product was a bright yellow solid and the yield was 95%. ^{1}H NMR (DMOS-d_6, 400 MHz, 298 K) δ: 7.70 (d, J = 9.06 Hz, 1H, Ar), 7.95 (s, 1H, Ar), 8.15 (dd, J = 8.98, 2.32 Hz, 1H, Ar), 8.28 (d, J = 2.36 Hz, 1H, Ar), 12.31 (br s, 1H, N-H). ^{13}C NMR (DMSO-d_6, 100 MHz, 298 K) δ: 59.6, 113.7, 117.7, 118.4, 130.0, 134.8, 140.3, 142.3. ESI–MS (+): calculated mass spectrum formula $C_8H_5IN_2O_2$ for M+Na: 310.9294; experimental mass spectrum: 310.9294.

Preparation of 3-iodo-5-nitroindolyl-2′-deoxyribose (3)

To an ice-chilled solution of (**2**) (700 mg, 2.4 mmol) dissolved in anhydrous acetonitrile (80 ml) was added NaH (173 mg, 7.2 mmol). The reaction mixture was then stirred at room temperature for an hour under argon prior to the addition of the Hoffer's chlorosugar, 1-α-chloro-3,5-di-(*O*-*p*-toluoyl)-2-deoxy-D-ribose (996 mg, 3.0 mmol), prepared as previously described (28), and was further stirred for 16 h. The solvent was then rota-evaporated under reduced pressure and the resulting crude product was immediately dissolved in anhydrous methanol (100 ml). To this solution was added anhydrous sodium methoxide until the pH is >12 and stirred at room temperature under argon atmosphere for 16 h. The solvent was evaporated under reduced pressure, and the crude product was purified by silica flash column chromatography using chloroform:methanol (90:10) as the eluent to yield 81% of bright yellow-orange solid. ^{1}H NMR (DMSO-d_6, 400 MHz, 298 K) δ: 2.25–2.31 (m, 2H, 2′-H), 3.48–3.59 (m, 2H, 5′-H), 3.83–3.86 (m, 1-H, 4′-H), 4.34–4.38 (m, 1H, 3′-H), 4.99 (*t*, J = 5.28 Hz, 1H, 5′-OH), 5.34 (d, J = 4.13 Hz, 1H, 3′-OH), 6.44 (t_{app}, J = 6.96 Hz, 1H, 1′-H), 7.89 (d, J = 9.07 Hz, 1H, Ar), 8.09 (dd, J = 9.13, 2.33 Hz, 1H, Ar), 8.12 (s, 1H, Ar), 8.16 (d, J = 2.36 Hz, 1H, Ar). ^{13}C NMR (DMSO-d_6, 100 MHz, 298 K) δ: 40.7, 61.6, 62.5, 71.4, 86.1, 88.5, 112.8, 118.0, 118.8, 130.9, 134.4, 139.9, 142.8. ESI–MS (+): calculated mass spectrum formula $C_{13}H_{13}IN_2NaO_5$ for M+Na: 426.9767; experimental mass spectrum: 426.9764.

Preparation of 3-[(trimethylsilyl)ethynyl]-5-nitroindolyl-2′-deoxyribose (4)

To a solution of (**3**) (250 mg, 0.60 mmol), $Pd(PPh_3)_2Cl_2$ (40 mg, 57 μmol) and CuI (27.6 mg, 147 μmol) dissolved in anhydrous THF (7.0 ml) was added triethylamine (0.24 ml, 1.7 mmol). To this reaction mixture was added dropwise trimethylsilylacetylene (0.42 ml, 2.9 mmol) over a period of 20 min and stirred at room temperature under argon for 3 h. The solvent was then evaporated under reduced pressure and the resulting oily residue was dissolved in EtOAc (50 ml) and washed with saturated KCl solution (50 ml). The organic layer was collected and further washed with 50 ml of 0.5 M EDTA (pH = 8.0), followed by another 50 ml of the saturated KCl solution. The organic layer was dried with $MgSO_4$, filtered through celite, and the solvent evaporated under reduced pressure to obtain a red-orange foam. The crude product was purified by silica flash column chromatography using ethyl acetate:methanol (90:10) as the eluent to yield 55% of red-orange foam. ^{1}H NMR (DMSO-d_6, 400 MHz, 298 K) δ: 0.27 [s, 9 H, $Si(CH_3)_3$], 2.27–2.33 (m, 2H, 2′-H), 3.49–3.60 (m, 2H, 5′-H), 3.84–3.87 (m, 1-H, 4′-H), 4.35–4.39 (m, 1H, 3′-H), 4.99 (t, J = 5.27 Hz, 1H, 5′-OH), 5.35 (d, J = 4.21 Hz, 1H, 3′-OH), 6.48 (t_{app}, J = 6.94 Hz, 1H, 1′-H), 7.93 (d_{app}, J = 9.07 Hz, 1H, Ar), 7.86 (dd, J = 9.09, 2.47 Hz, 1H, Ar), 8.28 (s, 1H, Ar), 8.39 (dd, J = 2.35, 0.36 Hz, 1H, Ar). ESI–MS (+): calculated mass spectrum formula $C_{18}H_{22}N_2O_5Si$ for M + H: 375.1376; experimental mass spectrum: 375.1384.

Preparation of 3-ethynyl-5-nitroindolyl-2′-deoxyribose (5)

To a degassed solution of (**4**) (120 mg) dissolved in anhydrous THF was added TBAF in THF (1.20 ml, 1 M) and stirred at room temperature under argon for 3 h. The

solvent was evaporated under reduced pressure and the resulting crude product was purified by silica flash column chromatography using ethyl acetate:methanol (90:10) as the eluent to yield 80% of reddish foam. ^{1}H NMR (DMSO-d_6, 400 MHz, 298 K) δ: 2.27–2.33 (m, 2H, 2′-H), 3.49–3.60 (m, 2H, 5′-H), 3.84-3.87 (m, 1-H, 4′-H), 4.35–4.39 (m, 1H, 3′-H), 4.37 (s, 1H, –C ≡ C–H), 5.00 (t, J = 5.53 Hz, 1H, 5′-OH), 5.34 (d, J = 4.34 Hz, 1H, 3′-OH), 6.47 (t_{app}, J = 6.73 Hz, 1H, 1′-H), 7.92 (d, J = 9.20 Hz, 1H, Ar), 8.11 (dd, J = 9.20, 2.34 Hz, 1H, Ar), 8.27 (s, 1H, Ar), 8.39 (d, J = 2.27 Hz, 1H, Ar). ^{13}C NMR (DMSO-d_6, 100 MHz, 298 K) δ: 40.5, 62.1, 71.1, 76.3, 84.6, 85.9, 88.3, 99.5, 112.7, 116.1, 118.7, 128.9, 134.1, 138.4, 142.6. ESI–MS (+): calculated mass spectrum formula $C_{15}H_{14}N_2O_5$ for M + Na: 325.0800; experimental mass spectrum: 325.0799. UV (MeOH) λ_{275} (nm): $\varepsilon = 37\,500\ cm^{-1}\ M^{-1}$.

Preparation of 3-ethynyl-5-nitroindolyl-2′-deoxyribose-5′-triphosphate (6)

This compound was prepared as previously described (22,29) using compound (**5**) as the starting material. The triphosphorylation process was initiated by forming the 5′-monophosphorodichloridated intermediate by the dropwise addition of $POCl_3$ in the reaction mixture containing (**5**) (0.07 mmol) and Proton Sponge (0.11 mmol) dissolved in 0.37 ml of trimethylphosphate pre-chilled at 0°C. The reaction was stirred for 2 h and monitored by TLC using the solvent system of 1-propanol:ammonium hydroxide:water (6:3:1). The reaction mixture was then spontaneously treated with 0.5 M DMF solution of tributylammonium pyrophosphate (0.37 mmol) and tributylamine (0.37 mmol) and stirred for 15 min at room temperature. 1 M TEAB was added to quench the reaction and stirred at room temperature for 2 h, then the crude product was evaporated by rota-evaporation under reduced pressure and purified by preparative reverse phase HPLC (mobile phase A: 0.1 M TEAB; B: 35% ACN in 0.1 M TEAB). The desirable nucleotide was lyophilized to dryness and characterized by mass spectrometry and ^{31}P NMR. The isolated yield was ∼30%. ^{31}P-NMR (D_2O, 162 MHz) δ: −5.4 (γ-P), −10.2 (α-P), −21.3 (β-P). HiRes ESI–MS (−): calculated mass spectrum formula $C_{15}H_{15}N_2O_{14}P_3$ for [M-H]: 540.9820; spectral mass spectrum: 540.9830.

Polymerization assays

All enzymatic assays were performed as previously described (14). Briefly, k_{cat} and K_m values were determined using pseudo-first order reaction conditions in which DNA polymerase (1 nM) was preincubated with DNA substrate (500 nM) in an assay buffer and mixed with variable concentrations of the nucleotide analog (0.10–500 μM) and 10 mM Mg^{2+}. Reactions were quenched with 200 mM EDTA at variable times (5–600 s) and analyzed using 20% denaturing polyacrylamide gel electrophoresis as previously described (30). Gel images were obtained and quantified using a PhosphorImager instrument. Product formation was calculated as described (13). Time courses in product formation were fit using Equation (1):

$$y = mt + b \quad (1)$$

y is the amount of product, m is the rate of the reaction, t is time, and b is the y-intercept. K_m and k_{cat} values were determined by fits of the data points to the Michaelis-Menten Equation (2):

$$\text{rate} = (k_{cat} * [\text{dNTP}])/(K_m + [\text{dNTP}]) \quad (2)$$

where k_{cat} is the maximal turnover number of the polymerase, K_m is the Michaelis constant for dNTP, and [dNTP] is the concentration of nucleotide substrate.

Elongation beyond the incorporated non-natural nucleotides was measured using single turnover conditions in which 500 nM polymerase and 250 nM DNA was mixed with nucleotide and Mg^{2+}. After four half-lives, an aliquot of the reaction was quenched with 350 mM EDTA to validate nucleotide insertion opposite the lesion. At this time, 500 μM dGTP was added to initiate elongation. Aliquots were quenched with EDTA at variable time points and analyzed via denaturing gel electrophoresis.

Detection of nucleotide incorporation via 'click' chemistry

In vitro 'clicking' reactions were performed by adding 25 μM non-natural nucleotide to a reaction cocktail containing ^{32}P radio-labeled DNA (500 nM), Mg^{2+} (10 mM) and DNA polymerase (10 nM) to initiate the reaction, and incubated at room temperature for 5 min. The reaction was then quenched through heat-inactivation at 90°C for 10 min and allowed to cool down to room temperature. An aliquot was then subjected to 'click' reaction at 37°C for 90 min by the addition of a cocktail containing AlexaFluor488-azide (10 μM) and $CuSO_4$ (10 μM) in a Tris-buffered saline solution with the reducing agent ascorbic acid. The Tris-buffered saline solvent and reducing agent were from a Click-iT^{TM} kit (Invitrogen). All concentrations listed are final concentrations from a stock solution of $CuSO_4$ (Sigma-Aldrich) prepared in water and AlexaFluor488-azide dye (Invitrogen) dissolved in DMSO. The AlexaFluor488 dye fluorescence was visualized using the Typhoon 9400 instrument (excitation laser: 488 nm, emission filter: 526 SP).

RESULTS

Synthesis of a 'clickable' non-natural nucleoside and nucleoside triphosphate

The synthetic approach outlined in Figure 1D was used to convert 5-NITP into a 'clickable' nucleotide designated 3-ethynyl-5-nitroindolyl-2′-deoxyribose-5′-triphosphate (3-Eth-5-NITP). This multi-step process begins with the installation of iodine at the 3-position of 5-nitroindole followed by *N*-glycosidic bond formation between 3-iodo-5-nitroindole and the Hoffer's chlorosugar using sodium hydride. Deprotection of the 3′- and 5′-hydroxyl moieties of the protected deoxyribose sugar was performed using Zemplén conditions (31). This reaction

yields the β-anomeric isomer as the primary product as confirmed by nuclear-Overhauser effect (NOE) difference experiment (NOE's of H-2, H-7, H-2′ and H-4′ upon irradiation of H-1′ as shown in Supplementary Figure S1). Furthermore, the presence of an apparent triplet (t_{app}) peak for the H-1′ resonance with a coupling constant of ~7.0 Hz in the ^{1}H NMR spectrum are also characteristics for the β-anomer of *N*-nucleosides (32). The iodine was then substituted with trimethylsilylacetylene using the Sonogashira reaction (33) and eventually deprotected to obtain the free ethynyl functional group using 1 M TBAF in THF. Conversion of 3-ethynyl-5-nitroindolyl-2′-deoxyribonucleoside to the corresponding triphosphate was accomplished by first reacting the nucleoside with $POCl_3$ to form the 5′-monophosphoro-dichloridated nucleoside intermediate which was then treated with pyrophosphate to form the nucleoside 5′-triphosphate. The crude product from this one-pot synthesis was purified via reverse-phase HPLC. The purified product was characterized by ^{31}P-NMR and high resolution mass-spectrometry. Complete details regarding the synthesis of this non-natural nucleotide are provided in Material and Methods, while details regarding their characterization are provided in Supplementary Figure S2.

Kinetic analyses for incorporating non-natural nucleotides

The kinetics of incorporating 3-Eth-5-NITP and 5-NITP opposite an abasic site and templating nucleobases (A, C, G and T) were next measured to evaluate if the ethynyl group influenced the efficiency and/or selectivity of nucleotide incorporation. All kinetic experiments used a defined DNA substrate containing an abasic site or any of the four natural nucleobases at position 14 of the template (Figure 2A). Denaturing gel electrophoresis images provided in Figure 2B show that 5-NITP and 3-Eth-5-NITP are both preferentially incorporated opposite an abasic site as opposed to undamaged DNA. The selectivity for incorporation was further quantified by defining the kinetic parameters, K_m, k_{cat} and k_{cat}/K_m, for incorporating 5-NITP and 3-Eth-5-NITP opposite the DNA lesion. Time courses in product formation were generated using pseudo-first order reaction conditions in which 1 nM of exonuclease-deficient DNA polymerase was incubated with 500 nM DNA substrate and mixed with variable concentrations of non-natural nucleotide and 10 mM Mg^{2+}. Figure 2C provides representative time courses for the incorporation of variable concentrations of 3-Eth-5-NITP opposite an abasic site. Each time course was fit to an equation for a straight line [Equation (1)] to define rates of nucleotide incorporation [We note that all time courses show *y*-intercepts that are higher than 0 at $\Delta t = 0$ s. This phenomenon reflects biphasic kinetic behavior and indicates that the first turnover of the polymerase is much faster than subsequent rounds of nucleotide incorporation opposite the lesion. Indeed, experiments performed using single-turnover conditions (polymerase concentration in excess versus DNA substrate) provide a rate constant 26 s^{-1} for incorporating 3-Eth-5-NITP opposite an abasic site (Supplementary Data). Note that the rate constant of 26 s^{-1} measured under single-turnover conditions is ~7-fold faster than the k_{cat} of 3.5 s^{-1} measured under steady-state conditions]. The resulting plot of rate versus 3-Eth-5-NITP concentration is hyperbolic (Figure 2D), and a fit of the data to the Michaelis–Menten equation yields a k_{cat} value of $3.5 \pm 0.3\ s^{-1}$, a K_m of 0.20 ± 0.07 μM, and a k_{cat}/K_m of $1.75*10^7\ M^{-1}s^{-1}$. Identical experiments performed with 5-NITP yield a k_{cat} of $6.8 \pm 0.6\ s^{-1}$, a K_m of 3.2 ± 0.9 μM, and a k_{cat}/K_m of $0.21*10^7\ M^{-1}s^{-1}$ (data not shown). Comparison of these kinetics parameters provided in Table 1 indicates that the catalytic efficiency of 3-Eth-5-NITP is ~10-fold higher than 5-NITP during TLS. The enhancement is caused by lowering of the K_m for the nucleotide that results from the introduction of the hydrophobic and pi-electron rich ethynyl moiety that amplifies the base-stacking potential of the non-natural nucleotide (14).

Identical kinetic experiments were performed to define the kinetic parameters for the incorporation of 3-Eth-5-NITP and 5-NITP opposite undamaged DNA. A summary of these kinetic parameters is provided in Table 1. In general, k_{cat}/K_m values measured for inserting 5-NITP opposite any templating nucleobase are 100- to 1500-fold lower than that measured for incorporation opposite the non-instructional abasic site. Similar results are obtained with 3-Eth-5-NITP as it is also incorporated opposite templating nucleobases ~200-fold less efficiently compared to insertion opposite the abasic site. Indeed, it is surprising that 3-Eth-5-NITP is even more selective than 5-NITP for insertion opposite the non-instructional lesion. The increase in selectivity reflects the inability of 3-Eth-5-NITP to be incorporated opposite pyrimidines coupled with its poor insertion opposite purines. The combined kinetic properties of efficient and selective incorporation by this non-natural nucleotide make it an excellent chemical probe to study the mechanism of TLS.

Extension kinetics

The ability of either non-natural nucleotide to be extended was examined using protocols outlined in Figure 2E. In these experiments, polymerase and DNA substrate were first mixed with 150 μM dATP, 5-NITP, or 3-Eth-5-NITP to initiate incorporation opposite the abasic site. After four half-lives (time required to obtain 95% mispair formation), 500 μM of dGTP was added to initiate elongation beyond the misincorporated nucleotide. Data provided in Figure 2F shows that dATP, when paired opposite the abasic site, is elongated rather efficiently. In contrast, neither 5-NITP nor 3-Eth-5-NITP is extendable when paired opposite an abasic site. As before, the lack of extension is interesting since both non-natural nucleotides are incorporated opposite this non-instructional DNA lesion with remarkably high catalytic efficiencies. The dichotomy between facile incorporation kinetics and poor elongation potential indicates that the biophysical features required for elongation are distinct from those needed for efficient incorporation opposite the non-instructional lesion.

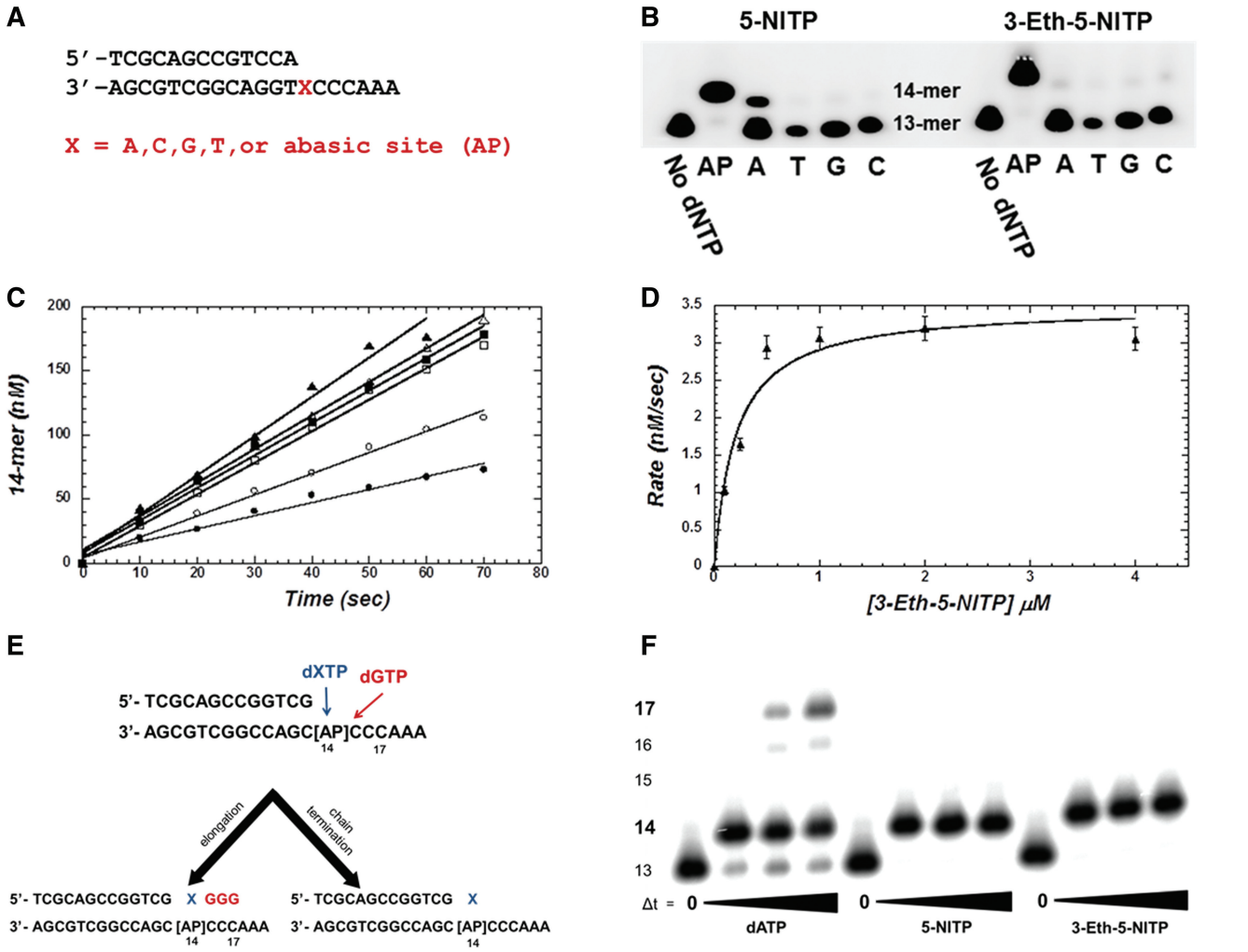

Figure 2. Validation that non-natural nucleotides are substrates during TLS. (**A**) DNA substrate used for kinetic analysis. (**B**) Denaturing gel electrophoresis image comparing the incorporation of 5-NITP (left) and 3-Eth-5-NITP (right) opposite an abasic site and templating bases (A, C, G and T). (**C**) Representative time courses for the incorporation of 3-Eth-5-NITP opposite an abasic site performed using 1 nM of the exonuclease-deficient bacteriophage T4 DNA polymerase, 500 nM 13/20AP DNA substrate, and 10 mM Mg^{2+} in a reaction buffer with the following 3-Eth-5-NITP concentrations: 0.10 (closed circle), 0.25 (open circle), 0.50 (open square), 1.0 (closed square), 2.0 (open triangle), or 4.0 μM (closed triangle) (**D**) Michaelis–Menten plot for the incorporation of 3-Eth-5-NITP opposite an abasic site yielded the following kinetic parameters: $k_{cat} = 3.5 \pm 0.3\,s^{-1}$, $K_m = 0.20 \pm 0.07\,\mu M$, $k_{cat}/K_m = 1.75*10^7\,M^{-1}\,s^{-1}$. (**E**) Experimental protocol used to evaluate the chain termination capabilities of the non-natural nucleotides used in this study. (**F**) Gel electrophoresis data evaluating incorporation and extension beyond an abasic site. Experiments were performed using single turnover conditions by mixing 500 nM DNA polymerase and 250 nM DNA with nucleotide and Mg^{2+}. After four half-lives, an aliquot of the reaction was quenched with 350 mM EDTA to validate nucleotide insertion opposite the lesion. At this time, 500 μM dGTP was added to initiate elongation. As indicated, dATP can be incorporated opposite the DNA lesion and extended. While 5-NITP and 3-Eth-5-NITP are incorporated opposite the DNA lesion, they are not extended and thus behave as chain terminators.

Table 1. Summary of kinetic parameters for the incorporation of 5-NITP and 3-Eth-5-NITP opposite an abasic site or templating nucleobases[a]

	5-NITP			3-Eth-5-NITP		
DNA	K_m [μM]	k_{cat} (s^{-1})	k_{cat}/K_m ($M^{-1}s^{-1}$)	K_m [μM]	k_{cat} (s^{-1})	k_{cat}/K_m ($M^{-1}s^{-1}$)
A	16 ± 6	0.39 ± 0.02	24 400	0.46 ± 0.07	0.041 ± 0.001	89 130
C	64 ± 6	0.072 ± 0.002	1130	ND[b]	ND	ND
G	8.7 ± 1.7	0.026 ± 0.002	2990	11.3 ± 5.2	0.094 ± 0.017	8320
T	22 ± 3	0.074 ± 0.002	3360	ND	ND	ND
Abasic	3.2 ± 0.9	6.8 ± 0.6	2 125 000	0.20 ± 0.07	3.5 ± 0.3	17 500 000

[a]Experiments were performed using the high-fidelity bacteriophage T4 DNA polymerase as a model DNA polymerase. Assays were performed as previously described (18).
[b]Not determined due to low amounts of product formed even at the highest concentration of nucleotide tested (500 μM).

Visualization of nucleotide incorporation using 'click' chemistry

We next tested the ability of this non-natural nucleotide to visualize TLS using 'click' chemistry to label the incorporated non-natural nucleotide with a fluorogenic reporter. First, 5-NITP or 3-Eth-5-NITP were enzymatically incorporated opposite an abasic site lesion and aliquots of the reaction were subjected to 'click' chemistry using AlexaFluor488-azide dye and Cu(I) formed *in situ* from Cu(II) with a reducing agent, ascorbic acid, in a tris-buffered saline solvent. Figure 3A shows representative denaturing gel electrophoresis data validating product formation. Lane 1 shows the 'clicking' reaction for DNA containing 3-Eth-5-NITP incorporated opposite the lesion. This sample contains two species with different mobilities: an upper band representing 'clicked' DNA and a lower band representing unreacted AlexaFluor488-azide. This conclusion is supported by the presence of a single fluorogenic species in 'clicking' reactions of DNA and 3-Eth-5-NITP in the absence of polymerase (lane 2) and AlexaFluor488-azide alone (lane 3).

The presence of 'clicked' DNA was also confirmed by radiolabeling the DNA from the reactions and using PhosphorImaging techniques to visualize the separated products after denaturing gel electrophoresis. Figure 3B shows that the reaction of 'clicked' DNA containing 3-ethynyl-5-nitroindolyl-2′-deoxyribose-5′-monophosphate (3-Eth-5-NIMP) at the primer terminus contains two species with different mobilities (lane 3). The upper band represents 'clicked' DNA while the lower band represents DNA that was elongated but that did not react with the AlexaFluor488-azide. Quantifying these products indicates that the efficiency of 'clicking' 3-Eth-5-NIMP in a DNA primer is ~30%. As before, the clicking reaction is absolutely dependent upon the presence of the ethynyl moiety as a 'clicked' species is not detected when 5-NITP is incorporated opposite the lesion (lane 6).

The ability of 3-Eth-5-NITP to selectively visualize the replication of an abasic site was further tested by performing the incorporation reaction in the presence of increasing concentrations of natural dNTPs. Experiments were performed mixing 40 nM DNA polymerase and 2 μM DNA substrate with 10 μM 3-Eth-5-NITP in the absence and presence of increasing dNTP concentrations (50–500 μM) in reaction buffer containing 10 mM Mg^{2+}. After incubation at room temperature for 60 s, the reactions were quenched by heating at 90°C for 10 min. The samples were allowed to cool to room temperature prior to 'clicking' of the non-natural nucleotide with AlexaFluor488-azide and Cu(I) for 2 h at 37°C. Samples were separated as described using denaturing polyacrylamide gel electrophoresis followed by washing of the gel with 20% methanol/water for 12 h. This washing step was included to remove unreacted AlexaFluor488-azide from the gel which serves to optimize the signal-to-noise ratio for detecting the labeled DNA. Gel electrophoresis data provided in Figure 3C reveals that the amount of fluorescently-labeled DNA remains essentially constant as the concentration of natural dNTPs is increased. Quantifying the amount of labeled DNA indicates that product formation is reduced by <5% even at 500 μM dNTPs, the highest concentration tested (data not shown). Collectively, the ability of 3-Eth-5-NITP to be incorporated opposite the lesion even in the presence of a 50-fold molar excess of natural nucleotides again highlights the incredibly high efficiency of the non-natural nucleotide for insertion opposite an abasic site.

Similar experiments were performed to further validate the selectivity of 3-Eth-5-NITP as a probe for damaged DNA. One key experiment measured the ability of natural nucleotides to inhibit the incorporation of 3-Eth-5-NITP opposite adenine (A) at position 14 in the template. Insertion opposite A was tested since previous kinetic analyses demonstrated that 3-Eth-5-NITP is incorporated opposite this natural nucleobase, albeit with poor efficiency (Table 1). Regardless, Figure 3D shows fluorescent labeling of 3-Eth-5-NITP after enzymatic insertion opposite A (lane 1). It is clear that the intensity of the 'clicked' nucleobase is significantly lower than that measured opposite an abasic site (lane 3). This reduced intensity is expected since 3-Eth-5-NITP is incorporated opposite templating DNA ~200-fold less efficiently than opposite the DNA lesion. More importantly, the addition of 10 μM dTTP completely inhibits the incorporation of 3-Eth-5-NITP opposite A (lane 2) but has no effect on the insertion of 3-Eth-5-NITP opposite an abasic site (lane 4). These results provide additional evidence for the selective nature of 3-Eth-5-NITP as a probe to measure the replication of non-instructional DNA lesions.

The final test for defining the selectivity of 3-Eth-5-NITP as a probe for TLS was to measure insertion opposite an abasic site when mixed with high concentrations of natural nucleotides. These experiments employed a 'running' start protocol using a DNA substrate with a primer nine bases upstream from the abasic site (Figure 4A). To optimize the extension reaction, assays were performed using single turnover conditions in which 500 nM bacteriophage T4 exo^- DNA polymerase was pre-incubated with 250 nM DNA (13/28AP-mer) followed by the addition of 500 μM dNTPs in the absence or presence of 10 μM 3-Eth-5-NITP. The control experiment performed with dNTPs alone shows that replication occurs up to and beyond the abasic site within 1 min (Figure 4B). The ability of the exonuclease-deficient DNA polymerase to bypass the abasic site at position 22 is consistent with previous reports (18). Reactions performed with dNTPs in the presence of 10 μM 3-Eth-5-NITP also show rapid synthesis up to the abasic site (Figure 4C). However, lesion bypass does not occur as replication products accumulate at the abasic site (position 22). The termination of DNA synthesis is undoubtedly caused by the selective incorporation of 3-Eth-5-NITP opposite the lesion. The chain terminating capabilities of 3-Eth-5-NITP are particularly impressive since these reactions were performed using a 50-fold molar excess of natural nucleotides, conditions which allow for facile elongation (Figure 4B). It should also be noted that DNA synthesis is terminated only at the abasic site and not at positions containing natural nucleobases. This last feature again highlights the

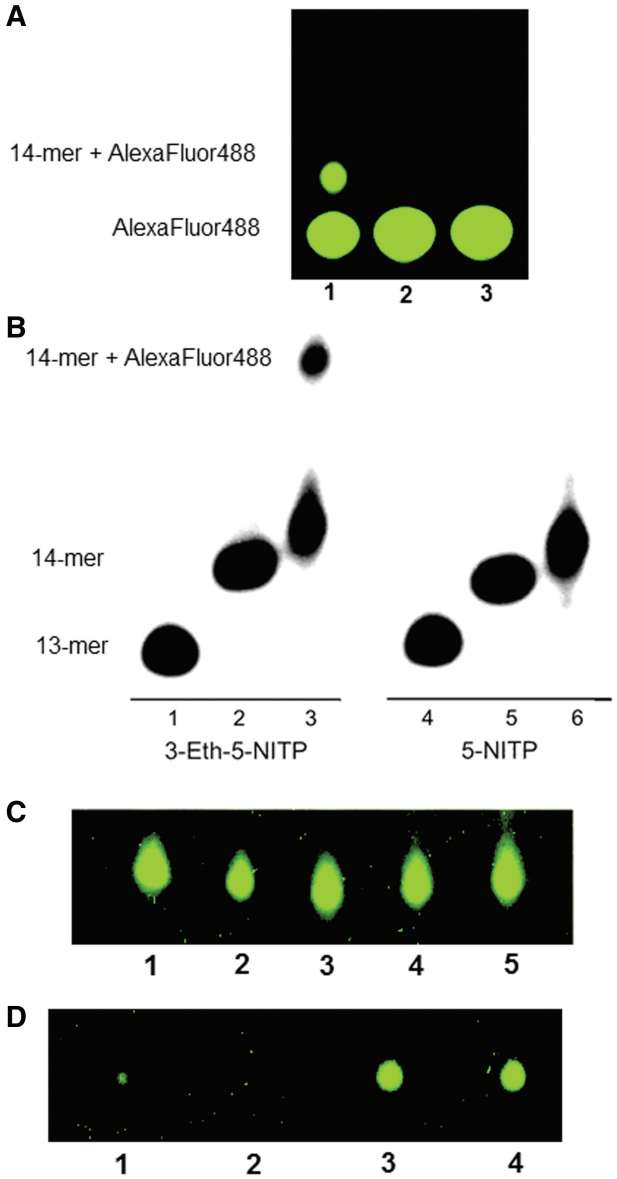

Figure 3. (**A**) Denaturing gel electrophoresis validates the ability of 3-Eth-5-NITP to react with an azide-containing fluorophore. Lane 1 shows the 'clicking' reaction of 3-Eth-5-NITP incorporated opposite abasic-containing DNA. The upper band represents 'clicked' DNA containing 3-Eth-5-NIMP while the lower band represents unreacted AlexaFluor488-azide. Lane 2 shows the presence of a single fluorogenic species in 'clicked' reactions of DNA and 3-Eth-5-NITP without DNA polymerase. Lane 3 shows AlexaFluor488-azide alone. (**B**) Autoradiogram of 'clicked' DNA. Lane 1 represents radiolabeled primer (13-mer) in the absence of polymerase and nucleotide substrate. Lane 2 represents the incorporation of 3-Eth-5-NITP opposite an abasic site. Lane 3 represents the 'clicking' reaction of DNA containing 3-Eth-5-NIMP opposite an abasic site. Lane 4 represents radiolabeled primer (13-mer) in the absence of polymerase and nucleotide substrate. Lane 5 represents the incorporation of 5-NITP opposite an abasic site. Lane 6 shows the 'clicking' reaction of DNA containing 5-NIMP opposite an abasic site. (**C**) Gel electrophoresis data showing the efficiency of 3-Eth-5-NITP incorporation opposite damaged DNA. Assays were performed using 40 nM bacteriophage T4 exo$^-$ DNA polymerase, 2 μM 13/20AP-mer DNA substrate in a buffer containing 10 mM Mg^{2+} and 10 μM 3-Eth-5-NITP in the presence of the following concentrations of dNTPs: 0 μM (lane 1), 50 μM (lane 2), 100 μM (lane 3), 250 μM (lane 4) and 500 μM (lane 5). (**D**) Denaturing gel electrophoresis validating the selectivity of 3-Eth-5-NITP for replicating damaged DNA. Assays were performed using

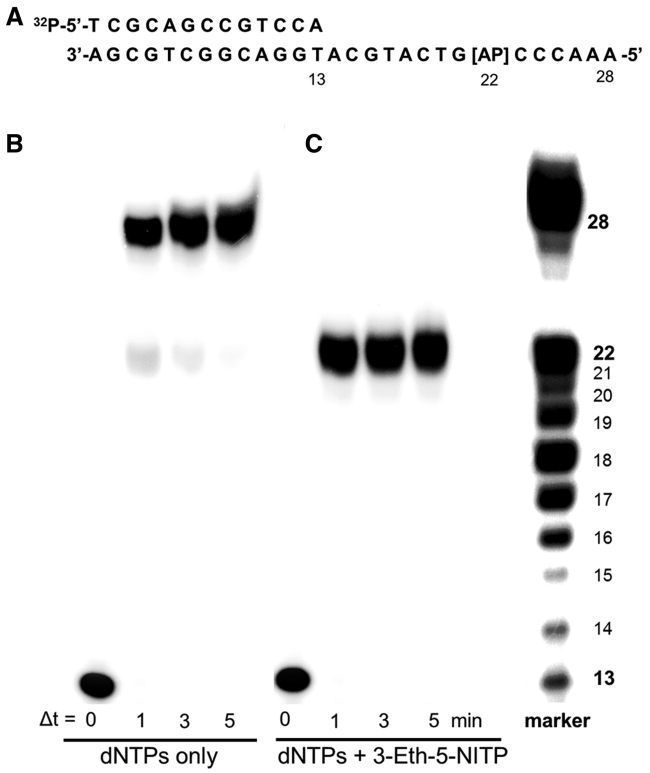

Figure 4. (**A**) DNA substrate used to analyze the selective incorporation of 3-Eth-5-NITP opposite an abasic site. (**B**) Denaturing gel electrophoresis demonstrating the ability of the bacteriophage T4 DNA polymerase to bypass an abasic site. Reactions were performed by pre-incubating 500 nM bacteriophage T4 exo$^-$ DNA polymerase with 250 nM 13/28AP-mer and initiating the reaction with 500 μM dNTPs. Although there is slight pausing at the lesion (position 22), the polymerase can completely elongate the DNA. (**C**) Denaturing gel electrophoresis validates the chain termination capabilities of 3-Eth-5-NITP during TLS. Reactions were performed by pre-incubating 500 nM bacteriophage T4 exo$^-$ DNA polymerase with 250 nM 13/28AP-mer and initiating the reaction with 500 μM dNTPs and 10 μM 3-Eth-5-NITP. Note that DNA synthesis is terminated specifically at the DNA lesion (position 22).

selectivity of 3-Eth-5-NITP as a substrate for the replication of damaged DNA.

DISCUSSION

At least 50 different types of DNA lesions have been identified both *in vitro* and *in vivo* (34,35). While most organisms possess sophisticated DNA repair pathways to correct damaged nucleic acid, these lesions frequently escape repair and are replicated in either a correct or error-prone process. In most cases, the ability of DNA polymerases to bypass a lesion has an immediate impact

40 nM bacteriophage T4 exo$^-$ DNA polymerase with the following conditions: 2 μM 13/20A-mer DNA substrate, 100 μM 3-Eth-5-NITP without dTTP (lane 1), 2 μM 13/20A-mer DNA substrate, 100 μM 3-Eth-5-NITP with 10 μM dTTP (lane 2), 2 μM 13/20AP-mer DNA substrate, 100 μM 3-Eth-5-NITP without dTTP (lane 3), or 2 μM 13/20AP-mer DNA substrate, 100 μM 3-Eth-5-NITP with 10 μM dTTP (lane 4).

of cell survival as it allows the continuity of cellular DNA synthesis to be maintained. There have been several recent reports that highlight the roles of different DNA polymerases in replicating damaged DNA (36–39). However, a clear understanding of TLS has been hindered due to the lack of chemical tools that can quantify this biological process at the molecular and cellular level. One glaring deficiency is the lack of nucleotide analogs that can be selectively and efficiently inserted opposite different forms of DNA damage. In this report, we describe the synthesis and application of a novel nucleotide that can monitor and quantify the ability of DNA polymerases to replicate a specific DNA lesion that is frequently formed under physiological conditions. Monitoring the replication of an abasic site is important since TLS can cause both beneficial and adverse cellular effects. For example, mutagenic DNA synthesis can drive evolutionary changes (40) or produce immunological diversity in higher organisms (41) which can be advantageous for an organism's survival. In contrast, TLS can produce adverse effects including the initiation of cancer in humans (42) as well as introducing mutations that cause drug resistance in microbial and viral species (43).

Herein, we show that 3-Eth-5-NITP is a prototypical non-natural nucleotide analog that can function as a chemical tool to accurately and selectively monitor the misreplication of an abasic site, a frequently formed non-instructional DNA lesion. In this respect, 3-Eth-5-NITP is incorporated opposite an abasic site 200- to 2000-fold more efficiently than opposite templating nucleobases. This selectivity is driven by poor insertion of 3-Eth-5-NITP opposite purines coupled with the lack of insertion opposite pyrimidines that are predicted to be complementary partners for this non-natural nucleotide. The unusual preference for incorporation opposite purines may be caused by changes in the *syn*- versus *anti*-configuration of the non-natural nucleotide as similar reports have been reported with modified purines such as 8-oxo-dATP and 8-oxo-dGTP (44,45). This conclusion is speculative and requires more advanced structural studies to confirm or refute its validity. Regardless, these data show that 3-Eth-5-NITP is a selective nucleotide for replicating an abasic site, and this activity has several potential applications. One possible use is as a chemical reagent to detect the replication of abasic sites present in large pieces of DNA such as genomic samples. While there are numerous types of DNA lesions, abasic sites are arguably the most prevalent as they form spontaneously at appreciable rates ranging from 10 000 to 200 000 per day per cell (4,5). Although antibodies (46) and small molecule reagents (47–49) can detect the presence of abasic sites in genomic DNA, the non-instructional nature of this lesion makes it extremely difficult to define the mutagenic consequences caused by its replication. The data here shows that 3-Eth-5-NITP can act as a sensitive probe to monitor the replication of this non-coding DNA lesion. We envision that combining 3-Eth-5-NITP with these lesion-specific probes will be useful in determining the fraction of lesions that are replicated by various DNA polymerases.

Similar pragmatic applications include detecting abasic sites in DNA during PCR amplification. Since abasic sites are strong blocks toward replication (7,18), this lesion can form abortive intermediates caused by inhibiting PCR-mediated synthesis. We note that while 3-Eth-5-NITP is a selective probe for the replication of abasic sites, its inability to be elongated prohibits its use as a nucleotide substrate for PCR-amplification of nucleic acid that contains abasic sites. However, we have demonstrated that other non-natural nucleotides such as 5-methylcarboxylate-indole-2′-deoxyriboside-5′-triphosphate (5-MeCITP) are incorporated opposite this non-instructional lesion almost as effectively as 5-NITP (13). Indeed, facile extension beyond the abasic site occurs when the nitro moiety is replaced with a functional group such as methyl carboxylate that provides hydrogen bonding interactions needed for elongation (13). Current efforts are underway to convert 5-MeCITP into a 'clickable' nucleotide analog that can fully replicate and quantify abasic site-containing DNA.

This study also paves the way to develop other nucleotide analogs that are specific to detect the misreplication of other DNA lesions. In this respect, we recently reported a novel analog, designated 4-methylpyrimidone-2′-deoxyriboside triphosphate (4-MePoTP), that is inserted opposite O^6-methylguanine ~100-fold more efficiently than opposite unmodified guanine or adenine (50). This high selectivity, coupled with its ability to be elongated indicates that it could be converted into a 'clickable' nucleotide to monitor the replication of miscoding DNA lesions such as O^6-methylguanine.

Perhaps the most challenging endeavor, however, will be to apply this type of non-natural nucleotide to study lesion bypass at the cellular level. It will be exciting to determine if the corresponding non-natural nucleoside can monitor TLS inside a cell. This would be an important advancement in cell biology as there is currently a lack of chemical tools that function as nucleotide substrates to accurately differentiate between correct versus mutagenic DNA synthesis.

SUPPLEMENTARY DATA

Supplementary Data are available at NAR Online: Supplementary Figures 1–3.

FUNDING

Funding for open access charge: National Institutes of Health (CA118408 to A.J.B.); the National Cancer Institute Training Programs in Cancer Pharmacology (CA148052 to E.A.M.). Funding for open access charge: NIH.

Conflict of interest statement. None declared.

REFERENCES

1. Hanawalt,P.C. (2007) Paradigms for the three rs: DNA replication, recombination, and repair. *Mol. Cell*, **28**, 702–707.

2. Pages,V. and Fuchs,R.P. (2002) How DNA lesions are turned into mutations within cells? *Oncogene*, **21**, 8957–8966.
3. Huffman,J.L., Sundheim,O. and Tainer,J.A. (2005) DNA base damage recognition and removal: new twists and grooves. *Mutat. Res.*, **577**, 55–76.
4. Atamna,H., Cheung,I. and Ames,B.N. (2000) A method for detecting abasic sites in living cells: age-dependent changes in base excision repair. *Proc. Natl Acad. Sci. USA*, **97**, 686–691.
5. Nakamura,J. and Swenberg,J.A. (1999) Endogenous apurinic/apyrimidinic sites in genomic DNA of mammalian tissues. *Cancer Res.*, **59**, 2522–2526.
6. Gates,K.S., Nooner,T. and Dutta,S. (2004) Biologically relevant chemical reactions of N7-alkylguanine residues in DNA. *Chem. Res. Toxicol.*, **17**, 839–856.
7. Boiteux,S. and Guillet,M. (2004) Abasic sites in DNA: repair and biological consequences in Saccharomyces cerevisiae. *DNA Repair*, **3**, 1–12.
8. Strauss,B.S. (2002) The "A" rule revisited: polymerases as determinants of mutational specificity. *DNA Repair*, **1**, 125–135.
9. Gentil,A., Cabral-Neto,J.B., Mariage-Samson,R., Margot,A., Imbach,J.L., Rayner,B. and Sarasin,A. (1992) Mutagenicity of a unique apurinic/apyrimidinic site in mammalian cells. *J. Mol. Biol.*, **227**, 981–984.
10. Loeb,L.A. (1998) Cancer cells exhibit a mutator phenotype. *Adv. Cancer Res.*, **72**, 25–56.
11. Nair,D.T., Johnson,R.E., Prakash,L., Prakash,S. and Aggarwal,A.K. (2011) DNA synthesis across an abasic lesion by yeast REV1 DNA polymerase. *J. Mol. Biol.*, **406**, 18–28.
12. Choi,J.Y., Lim,S., Kim,E.J., Jo,A. and Guengerich,F.P. (2010) Translesion synthesis across abasic lesions by human B-family and Y-family DNA polymerases alpha, delta, eta, iota, kappa, and REV1. *J. Mol. Biol.*, **404**, 34–44.
13. Motea,E.A., Lee,I. and Berdis,A.J. (2011) Quantifying the energetic contributions of desolvation and pi-electron density during translesion DNA synthesis. *Nucleic Acids Res.*, **39**, 1623–1637.
14. Reineks,E.Z. and Berdis,A.J. (2004) Evaluating the contribution of base stacking during translesion DNA replication. *Biochemistry*, **43**, 393–404.
15. Vineyard,D., Zhang,X., Donnelly,A., Lee,I. and Berdis,A.J. (2007) Optimization of non-natural nucleotides for selective incorporation opposite damaged DNA. *Org. Biomol. Chem.*, **5**, 3623–3630.
16. Zhang,X., Lee,I. and Berdis,A.J. (2004) Evaluating the contributions of desolvation and base-stacking during translesion DNA synthesis. *Org. Biomol. Chem.*, **2**, 1703–1711.
17. Sheriff,A., Motea,E., Lee,I. and Berdis,A.J. (2008) Mechanism and dynamics of translesion DNA synthesis catalyzed by the Escherichia coli Klenow fragment. *Biochemistry*, **47**, 8527–8537.
18. Berdis,A.J. (2001) Dynamics of translesion DNA synthesis catalyzed by the bacteriophage T4 exonuclease-deficient DNA polymerase. *Biochemistry*, **40**, 7180–7191.
19. Zahn,K.E., Belrhali,H., Wallace,S.S. and Doublie,S. (2007) Caught bending the A-rule: crystal structures of translesion DNA synthesis with a non-natural nucleotide. *Biochemistry*, **46**, 10551–10561.
20. Loakes,D. and Brown,D.M. (1994) 5-Nitroindole as an universal base analogue. *Nucleic Acids Res.*, **22**, 4039–4043.
21. Smith,C.L., Simmonds,A.C., Hamilton,A.L., Martin,D.L., Lashford,A.G., Loakes,D., Hill,F. and Brown,D.M. (1998) Use of 5-nitroindole-2'-deoxyribose-5'-triphosphate for labelling and detection of oligonucleotides. *Nucleos. Nucleot.*, **17**, 555–564.
22. Smith,C.L., Simmonds,A.C., Felix,I.R., Hamilton,A.L., Kumar,S., Nampalli,S., Loakes,D., Hill,F. and Brown,D.M. (1998) DNA polymerase incorporation of universal base triphosphates. *Nucleos. Nucleot.*, **17**, 541–554.
23. Kolb,H.C. and Sharpless,K.B. (2003) The growing impact of click chemistry on drug discovery. *Drug. Discov. Today*, **8**, 1128–1137.
24. Nwe,K. and Brechbiel,M.W. (2009) Growing applications of "click chemistry" for bioconjugation in contemporary biomedical research. *Cancer Biother. Radiopharm.*, **24**, 289–302.
25. Huber,C.G. and Krajete,A. (2000) Sheath liquid effects in capillary high-performance liquid chromatography-electrospray mass spectrometry of oligonucleotides. *J. Chromatogr. A*, **870**, 413–424.
26. Capson,T.L., Peliska,J.A., Kaboord,B.F., Frey,M.W., Lively,C., Dahlberg,M. and Benkovic,S.J. (1992) Kinetic characterization of the polymerase and exonuclease activities of the gene 43 protein of bacteriophage T4. *Biochemistry*, **31**, 10984–10994.
27. Rush,J. and Konigsberg,W.H. (1989) Rapid purification of overexpressed T4 DNA polymerase. *Prep. Biochem.*, **19**, 329–340.
28. Rolland,V., Kotera,M. and Lhomme,J. (1997) Convenient Preparation of 2-Deoxy-3,5-di-O-p-toluoyl-α-D-erythro-pentofuranosyl Chloride. *Syn. Communicat.*, **27**, 3505–3511.
29. Zhang,X., Lee,I., Zhou,X. and Berdis,A.J. (2006) Hydrophobicity, shape, and pi-electron contributions during translesion DNA synthesis. *J. Am. Chem. Soc.*, **128**, 143–149.
30. Mizrahi,V., Benkovic,P. and Benkovic,S.J. (1986) Mechanism of DNA polymerase I: exonuclease/polymerase activity switch and DNA sequence dependence of pyrophosphorolysis and misincorporation reactions. *Proc. Natl Acad. Sci. USA*, **83**, 5769–5773.
31. Thompson,A. and Wolfrom,M.L. (1963) *Methods in Carbohydrate Chemistry*. Academic Press, Inc., New York.
32. Ren,R.X., Chaudhuri,N.C., Paris,P.L., Rumney,S. and Kool,E.T. (1996) Naphthalene, phenanthrene, and pyrene as DNA base analogues: synthesis, structure, and fluorescence in DNA. *J. Am. Chem. Soc.*, **118**, 7671–7678.
33. Sonogashira,K., Tohda,Y. and Hagihara,N. (1975) A convenient synthesis of acetylenes: catalytic substitutions of acetylenic hydrogen with bromoalkenes, iodoarenes and bromopyridines. *Tetrahedron Lett.*, **16**, 4467–4470.
34. Cadet,J., Delatour,T., Douki,T., Gasparutto,D., Pouget,J.P., Ravanat,J.L. and Sauvaigo,S. (1999) Hydroxyl radicals and DNA base damage. *Mutat. Res.*, **424**, 9–21.
35. Sedgwick,B., Bates,P.A., Paik,J., Jacobs,S.C. and Lindahl,T. (2007) Repair of alkylated DNA: recent advances. *DNA Repair*, **6**, 429–442.
36. Crespan,E., Amoroso,A. and Maga,G. (2010) DNA polymerases and mutagenesis in human cancers. *Subcell. Biochem.*, **50**, 165–188.
37. Cruet-Hennequart,S., Gallagher,K., Sokol,A.M., Villalan,S., Prendergast,A.M. and Carty,M.P. (2010) DNA polymerase eta, a key protein in translesion synthesis in human cells. *Subcell. Biochem.*, **50**, 189–209.
38. Kunkel,T.A. (2009) Evolving views of DNA replication (in)fidelity. *Cold Spring Harb. Symp. Quant. Biol.*, **74**, 91–101.
39. Zahn,K.E., Wallace,S.S. and Doublie,S. (2011) DNA polymerases provide a canon of strategies for translesion synthesis past oxidatively generated lesions. *Curr. Opin. Struct. Biol.*, **21**, 358–369.
40. Long,M. (2001) Evolution of novel genes. *Curr. Opin. Genet. Dev.*, **11**, 673–680.
41. Gearhart,P.J. and Wood,R.D. (2001) Emerging links between hypermutation of antibody genes and DNA polymerases. *Nat. Rev. Immunol.*, **1**, 187–192.
42. Prindle,M.J., Fox,E.J. and Loeb,L.A. (2010) The mutator phenotype in cancer: molecular mechanisms and targeting strategies. *Curr. Drug Targets*, **11**, 1296–1303.
43. Lerma,J.G.G. and Heneine,W. (2001) Resistance of human immunodeficiency virus type 1 to reverse transcriptase and protease inhibitors: genotypic and phenotypic testing. *J. Clin. Virol.*, **21**, 197–212.
44. Patro,J.N., Urban,M. and Kuchta,R.D. (2009) Interaction of human DNA polymerase alpha and DNA polymerase I from Bacillus stearothermophilus with hypoxanthine and 8-oxoguanine nucleotides. *Biochemistry*, **48**, 8271–8278.
45. Purmal,A.A., Kow,Y.W. and Wallace,S.S. (1994) 5-Hydroxypyrimidine deoxynucleoside triphosphates are more efficiently incorporated into DNA by exonuclease-free Klenow fragment than 8-oxopurine deoxynucleoside triphosphates. *Nucleic Acids Res.*, **22**, 3930–3935.
46. Chen,B.X., Kubo,K., Ide,H., Erlanger,B.F., Wallace,S.S. and Kow,Y.W. (1992) Properties of a monoclonal antibody for the

detection of abasic sites, a common DNA lesion. *Mutat. Res.*, **273**, 253–261.
47. Jakobsen,U., Shelke,S.A., Vogel,S. and Sigurdsson,S.T. (2010) Site-directed spin-labeling of nucleic acids by click chemistry: detection of abasic sites in duplex DNA by EPR spectroscopy. *J. Am. Chem. Soc.*, **132**, 10424–10428.
48. Kojima,N., Takebayashi,T., Mikami,A., Ohtsuka,E. and Komatsu,Y. (2009) Construction of highly reactive probes for abasic site detection by introduction of an aromatic and a guanidine residue into an aminooxy group. *J. Am. Chem. Soc.*, **131**, 13208–13209.
49. Wang,Y., Liu,L., Wu,C., Bulgar,A., Somoza,E., Zhu,W. and Gerson,S.L. (2009) Direct detection and quantification of abasic sites for in vivo studies of DNA damage and repair. *Nucleic Med. Biol.*, **36**, 975–983.
50. Chavarria,D., Ramos-Serrano,A., Hirao,I. and Berdis,A.J. (2011) Exploring the roles of nucleobase desolvation and shape complementarity during the misreplication of O6-methylguanine. *J. Mol. Biol.*, **412**, 325–339.